NACA TN 2172 /6958

TECH LIBRARY KAFB, NM
0065170

NATIONAL ADVISORY COMMITTEE FOR AERONAUTICS

TECHNICAL NOTE 2172

LOW-SPEED INVESTIGATION OF THE STALLING OF A THIN, FAIRED, DOUGLE-WEDGE AIRFOIL WITH NOSE FLAP

By Leonard M. Rose and John M. Altman

Ames Aeronautical Laboratory
Moffett Field, Calif.

Washington
August 1950

TECH LIBRARY KAFB, NM

0065170

NATIONAL ADVISORY COMMITTEE FOR AERONAUTICS

TECHNICAL NOTE 2172

LOW-SPEED INVESTIGATION OF THE STALLING OF A THIN, FAIRED, DOUBLE-WEDGE AIRFOIL WITH NOSE FLAP

By Leonard M. Rose and John M. Altman

SUMMARY

The stalling characteristics of a 4.23-percent-thick, faired, double-wedge airfoil section with and without a plain nose flap were investigated. Flap chords equal to 12, 16, 20, and 25 percent of the airfoil chord were tested. Results of force and pressure-distribution measurements as well as studies of the boundary layer are presented for a Reynolds number of 5,800,000 and a Mach number of 0.17.

The basic airfoil section stalled as a result of separation of flow from the entire upper surface. The flow separation first occurred at the leading edge at a small angle of attack and was followed by reattachment of the flow to the surface a short distance downstream. The chordwise extent of separated flow increased with increase in angle of attack until the flow was separated from the entire upper surface at the initial lift peak. With the nose flap deflected, the separation of the flow was delayed to higher angles of attack. With the nose flap deflected 20° or less, the stall was similar to that for the basic airfoil. For nose-flap deflections greater than 20°, flow separation starting from the trailing edge was also encountered and maximum lift was determined by combined leading- and trailing-edge separation. No significant differences in stalling characteristics were noted for the range of flap-chord ratios investigated.

INTRODUCTION

Because of the increased interest in thin airfoil sections for use on high-speed airplanes, a low-speed investigation of the manner in which such airfoil sections stall is being conducted in the Ames 7- by 10-foot wind tunnels. The investigation has been directed toward gaining an understanding of the mechanism of the stall of these sections with the hope that such knowledge would lead to means for improving the characteristics of wings. Results have been presented for airfoils of NACA 6-series sections having maximum thicknesses equal to 6 and 9 percent of the chord (references 1 and 2). This report presents the results of such an investigation of a 4.23-percent-thick, sharp-edged, faired, double-wedge section.

Since the characteristics of thin, sharp-edged airfoils were known to be improved by the use of plain nose flaps, this investigation dealt to a considerable extent with the effects of a nose flap on the stalling characteristics, and with the effects of this flap on the forces and moments of the airfoil section. Results of the force and moment phase can be found in references 3 and 4.

NOTATION

The results are presented in the form of standard NACA coefficients which are defined as follows:

c_d section drag coefficient $\left(\frac{d}{qc}\right)$

c_l section lift coefficient $\left(\frac{l}{qc}\right)$

c_m section pitching-moment coefficient, referred to the quarter-chord point $\left(\frac{m}{qc^2}\right)$

c airfoil chord, feet

d drag per unit span, pounds per foot

l lift per unit span, pounds per foot

m pitching moment per unit span, pound-feet per foot

P pressure coefficient $\left(\frac{p-p_o}{q}\right)$

p local static pressure, pounds per square foot

p_o free-stream static pressure, pounds per square foot

q free-stream dynamic pressure $\left(\frac{1}{2}\rho_o U_o^2\right)$, pounds per square foot

U local velocity outside boundary layer, feet per second

U_o free-stream velocity, feet per second

u local velocity in boundary layer, feet per second

x distance along chord measured from leading edge, feet

y distance above surface measured normal to surface, feet

α_o section angle of attack, degrees

δ_n nose-flap deflection, degrees

ρ_o free-stream mass density, slugs per cubic foot

Subscript

u uncorrected coefficients

MODEL, APPARATUS, AND TESTS

The main portion of the model used in this investigation was built of wood on a steel spar and was covered with a thin aluminum skin. The flaps were constructed of solid metal in order that the leading-edge thickness could be maintained as small as practicable. The airfoil section was derived from a symmetrical double-wedge section that had a maximum thickness equal to 4.5 percent of the chord. The midchord portions of the upper and lower surfaces were rounded with arcs of a circle tangent to the 42.5- and 57.5-percent-chord stations. Nose flaps having chords equal to 12, 16, 20, and 25 percent of the airfoil chord were investigated. The flaps were connected to the model by a continuous hinge, and rubbing contact was maintained between the deflected flap and the skirt on the fixed portion of the airfoil. A section drawing of the model is shown in figure 1. Flush orifices were provided in the surface of the model at midspan for the measurement of pressure distribution.

The model spanned the 7-foot dimension of the wind-tunnel test section; the tips were attached to 6-foot-diameter turntables flush with the upper and lower walls. The lift, drag, and pitching-moment data were obtained by the use of the wind-tunnel balance system.

The velocity distributions above the wing were calculated from surveys of the static and total pressures above the surface of the model. Rakes made of small-diameter steel tubing were used for these surveys. As was discussed in reference 1, this method of measurement is subject to certain limitations; however, lack of better equipment precluded more precise measurements. The apparatus shown in figure 2 was used for transmitting rake pressures to multiple manometers; this apparatus was employed to avoid the necessity of attaching the pressure leads to the surface of the model. Surface static-pressure measurements made with and without the device in the tunnel indicated little effect on the surface pressure distribution.

All the data were obtained at a Reynolds number of 5.8 million and a Mach number of approximately 0.17.

CORRECTIONS

The results obtained from the wind-tunnel balance system include the forces and moments acting on the two turntables. With the exception of the drag, the effects of these turntables on the results have been found to be negligible; however, the drag results are in error due to the direct drag and interference drag of the turntables. As was discussed in reference 3, attempts to establish a drag tare for all test conditions were unsuccessful.

Although the results presented in references 3 and 4 were corrected for effects of the tunnel walls, the uncorrected results are presented herein in order that the force and moment data may be compared directly with the pressure-distribution and boundary-layer measurements. The magnitudes of the wall effects involved are listed as follows as derived from reference 5:

$$\Delta\alpha = 0.4755c_{l_u} + 1.903c_{m_u}$$

$$c_l = 0.941c_{l_u}$$

$$c_d = 0.9928c_{d_u}$$

$$c_m = 0.9939c_{m_u} + 0.0132c_{l_u}$$

RESULTS AND DISCUSSION

Results are presented in figures 3 to 6 for the basic airfoil section.

Comparison of the results for the flaps of various chords indicated no significant differences in the flow characteristics attributable to variation in flap chord. For this reason no comparison of the data for flaps of various chords is presented. The results in figures 7 to 12 illustrating the effects of flap deflection are for the flap of 12-percent chord with the exception of figure 10, which is for the 16-percent-chord flap.

Basic Airfoil

Force characteristics.– The force characteristics of the basic airfoil have been presented and discussed in reference 3. However, it is believed of interest to include in this report the results of further tests of the basic section wherein the angle of attack was increased well into the stalled region[1] and then reduced to obtain an indication of the stall-recovery characteristics of this airfoil section. These results are presented in figure 3. The force and moment coefficients for increasing and decreasing angle of attack indicated little hysteresis in the re-establishment of the prestall flow conditions. The results shown in this figure also indicate that large negative pitching moments and relatively small losses in lift followed the stall.

Pressure distribution.– The pressure distribution on the airfoil is shown in figure 4. For some angles of attack, the pressures close to the lower surface have been omitted in the figure for clarity. It should be noted that, as the angle of attack was increased from a small positive value, a region of essentially constant pressure occurred behind the leading edge, and, as the angle of attack was increased further, this region extended over a larger portion of the chord. The negative pressure coefficients were much smaller than those on thicker round-nose airfoils. The low value of the minimum pressure peak, together with the constant-pressure region, indicates that separation occurred at the leading edge. The low velocities around the nose of the section, as indicated by the pressures, account for the extreme variation of drag with lift evident in the force tests. These low velocities resulted in the realization of only a small part of the suction force normally encountered at the nose of most airfoils. The behavior of the region of essentially constant pressure immediately behind the leading edge also accounts for the variation of pitching-moment coefficient with lift coefficient shown in figure 3. As the lift coefficient was increased from zero, the load over the forward part of the airfoil increased much more rapidly than the load over the remainder of the chord until the constant-pressure region extended aft of the moment center (c/4). As the lift coefficient was then further increased, the load over the rear of the airfoil increased more rapidly, thereby resulting in increasingly negative pitching moments as the lift increased.

Flow studies.– The flow studies were made utilizing short tufts of thread glued to the surface of the model, as well as by surveys of the static and total pressures close to the surface. The pressure surveys indicated that the extent of the retarded flow above the wing was considerably greater than that encountered on round-nose airfoils. In

[1]In this report the stall is considered to correspond to conditions which exist following the first lift peak.

figure 5 the local-velocity ratio (u/U) above the wing is shown for an angle of attack of 6°. Immediately evident in this figure is the considerable extent of the separated region behind the leading edge. Tuft observations for this condition indicated a region of reversed or upstream flow extending approximately from 40-percent chord forward to 10-percent chord. The static-pressure surveys within this separated region were suggestive of a vortex flow. A further attempt to establish the existence of a vortex in this region by ejecting smoke from the surface of the model indicated only that a rotary flow existed. From the surveys of the flow close to the surface, it was possible to define both the height above the surface and the chordwise extent of the separated region. These results are shown in figure 6. Although no separated region is shown for angles of attack less than 3° in this figure, the pressure-distribution studies and the tuft observations indicated the existence of such a region for angles of attack of 1° and 2°. Although the precise point of separation could not be determined, apparently the flow left the nose of the airfoil and expanded back to the surface under the influence of the approaching stream. As the angle of attack was increased, the chordwise distance required for this expansion and reattachment to the surface increased until this distance exceeded the chord of the airfoil.

Effect of Nose-Flap Deflection

Force characteristics.- The force characteristics of the model with the nose flap deflected have been presented in reference 4; however, to facilitate comparisons, some of the lift and moment characteristics of the airfoil with the 12-percent-chord flap are presented in figure 7. In making comparisons of the data presented in this report with the results in reference 4, it should be remembered that the results herein have not been corrected for the effects of the wind-tunnel walls.

Pressure distribution.- Upper-surface pressure-distribution measurements with the nose flap deflected are compared in figure 8 for approximately zero lift, one-third and two-thirds $C_{l_{max}}$, and $C_{l_{max}}$. From this comparison, the essential effects of nose-flap deflection are evident. At low lift coefficients, deflection of the nose flap caused the stagnation point to be on the upper surface of the flap and the minimum pressure point to be near the flap hinge line. At some angle of attack, depending upon the flap deflection, the stagnation point moved to the lower surface. When the stagnation point moved to the lower surface, a region of relatively constant pressure developed on the upper surface near the leading edge. This region, which is characteristic of separated flow, became more apparent as the angle of attack was further increased. The location of the stagnation point as a function of the angle of attack, from examination of a large number of pressure distributions, is summarized in figure 9 for some of the flap deflections investigated.

With the nose flap deflected 35°, it was not possible to obtain pressure-distribution measurements that correlated with the force measurements. The data obtained indicated that the pressure distribution for a flap deflection of 35° was generally similar to that for the other flap deflections before the stagnation point moved to the lower surface. At greater angles of attack, however, it was possible to obtain two different types of load distributions at the same angle of attack under seemingly identical test conditions. These two types of distribution are shown in figure 10 for an angle of attack of 14°. For the condition noted as A in this figure, it is probable that the boundary layer over the flap remained laminar and that the flow was unable to negotiate the juncture between the flap and the afterportion of the airfoil without separation. For this condition, the maximum lift was lower than that obtained with 30° flap deflection. For condition B, the data for higher angles of attack (not included) indicate a relatively constant-pressure region immediately behind the leading edge which probably existed at 14°. Such regions indicate local separation which undoubtedly caused the flow to approach the flap juncture with a turbulent boundary layer better able to withstand the adverse pressure gradient in this region. For this condition, the maximum lift was higher than with 30° deflection. Although extensive pressure measurements with the 35° deflection of the flap were made only with the 16-percent-chord flap, the force and moment measurements indicated that similar conditions existed for the other flap chords investigated.

Flow studies.- The tuft observations of the flow near the surface indicated that separation occurred from the leading edge, as was the case for the flap undeflected. For the smaller flap deflections (i.e., less than 20°), the separated region increased in extent from the leading edge in a manner much like the growth of the separated region with the flap undeflected. The principal effect of small flap deflection was to delay the onset of separation to greater angles of attack. These tuft observations were substantiated by the velocity surveys near the surface. The extent of the separated region as a function of angle of attack, determined from the surveys, is shown in figure 11 for various flap deflections. These results indicate that as the flap was deflected the rate of growth of the separated region with angle of attack was decreased except near maximum lift where the rate of growth was much faster.

For flap deflections greater than 20°, it was found that trailing-edge separation also occurred near maximum lift. Because of the inability to repeat the characteristics with a flap deflection of 35°, it was not possible to obtain consistent enough results to define the extent of the separated region for this flap angle. The results obtained indicated that for the high-lift condition (case B in fig. 10) the stall occurred in a manner similar to the stall with the 30° flap deflection. For the low-maximum-lift case (case A in fig. 10), the results indicated that separation occurred at the trailing edge and no evidence of leading-edge separation was found. It is believed that further research on the characteristics of flow about a sharp edge is necessary before the behavior of the model with the flap deflected 35° can be fully understood.

For each flap deflection, as the angle of attack was increased a range was found where the boundary layer at a given station aft of the hinge line on the upper surface abruptly became thinner. The magnitude of this thinning for a flap deflection of 30° is shown in figure 12. Probably the reason for this reduction in boundary-layer thickness was the movement of the stagnation point to the lower surface of the airfoil, since this occurred prior to the thinning of the boundary layer. Prior to the movement of the stagnation point to the lower surface and the occurrence of flow separation at the nose, the boundary layer approaching the minimum pressure peak at the flap juncture was laminar. In traversing the flap-wing juncture, the flow was separated for a short distance along the surface, causing the boundary layer to grow rapidly, as shown in figure 12. After the movement of the stagnation point to the lower surface, the growth of the now-turbulent boundary layer near the flap juncture was markedly less.

With the occurrence of flow separation at the leading edge of the airfoil and the subsequent reattachment of the flow farther along the chord, the resulting boundary layers were considerably different than have been found previously for thicker round-nose airfoils. For this reason, attempts to analyze the boundary-layer growth in terms of the usual boundary-layer parameters proved fruitless. Although detailed measurements were not made near the point at which separation first occurred, it is not believed that the mechanism of the separation was the same as that found for the round-nose airfoils reported in references 1 and 2.

CONCLUDING REMARKS

The investigation of the manner of stalling of the faired, double-wedge airfoil equipped with plain nose flaps having chords equal to 12, 16, 20, and 25 percent of the airfoil chord showed the following:

The basic airfoil section stalled as a result of flow separation from the entire upper surface of the airfoil. The separation was first evident at the leading edge at a small positive angle of attack. As the angle of attack was increased, the distance required for the separated flow to reattach to the surface increased. The initial lift peak was obtained when the flow reattachment point coincided with the trailing edge.

For nose-flap deflections of 20° and less, the stall was similar to the stall of the basic section. For flap deflections greater than 20°, flow separation starting from the trailing edge was also encountered near maximum lift. The effect of nose-flap deflection was to delay the onset

of the leading-edge separation to higher angles of attack. No significant differences in stalling characteristics were noted with variations in flap-chord ratio from 12 to 25 percent of the airfoil chord.

Ames Aeronautical Laboratory,
National Advisory Committee for Aeronautics,
Moffett Field, Calif., May 25, 1950.

REFERENCES

1. McCullough, George B., and Gault, Donald E.: Boundary-Layer and Stalling Characteristics of the NACA 64A006 Airfoil Section. NACA TN 1923, 1949.

2. Gault, Donald E.: Boundary-Layer and Stalling Characteristics of an NACA 63-009 Airfoil Section. NACA TN 1894, 1949.

3. Rose, Leonard M., and Altman, John M.: Low-Speed Experimental Investigation of a Thin, Faired, Double-Wedge Airfoil Section with Nose and Trailing-Edge Flaps. NACA TN 1934, 1949.

4. Rose, Leonard M., and Altman, John M.: Low-Speed Investigation of a Thin, Faired, Double-Wedge Airfoil Section with Nose Flaps of Various Chords. NACA TN 2018, 1950.

5. Allen, H. Julian, and Vincenti, Walter G.: Wall Interference in a Two-Dimensional-Flow Wind Tunnel, with Consideration of the Effects of Compressibility. NACA Rep. 782, 1944.

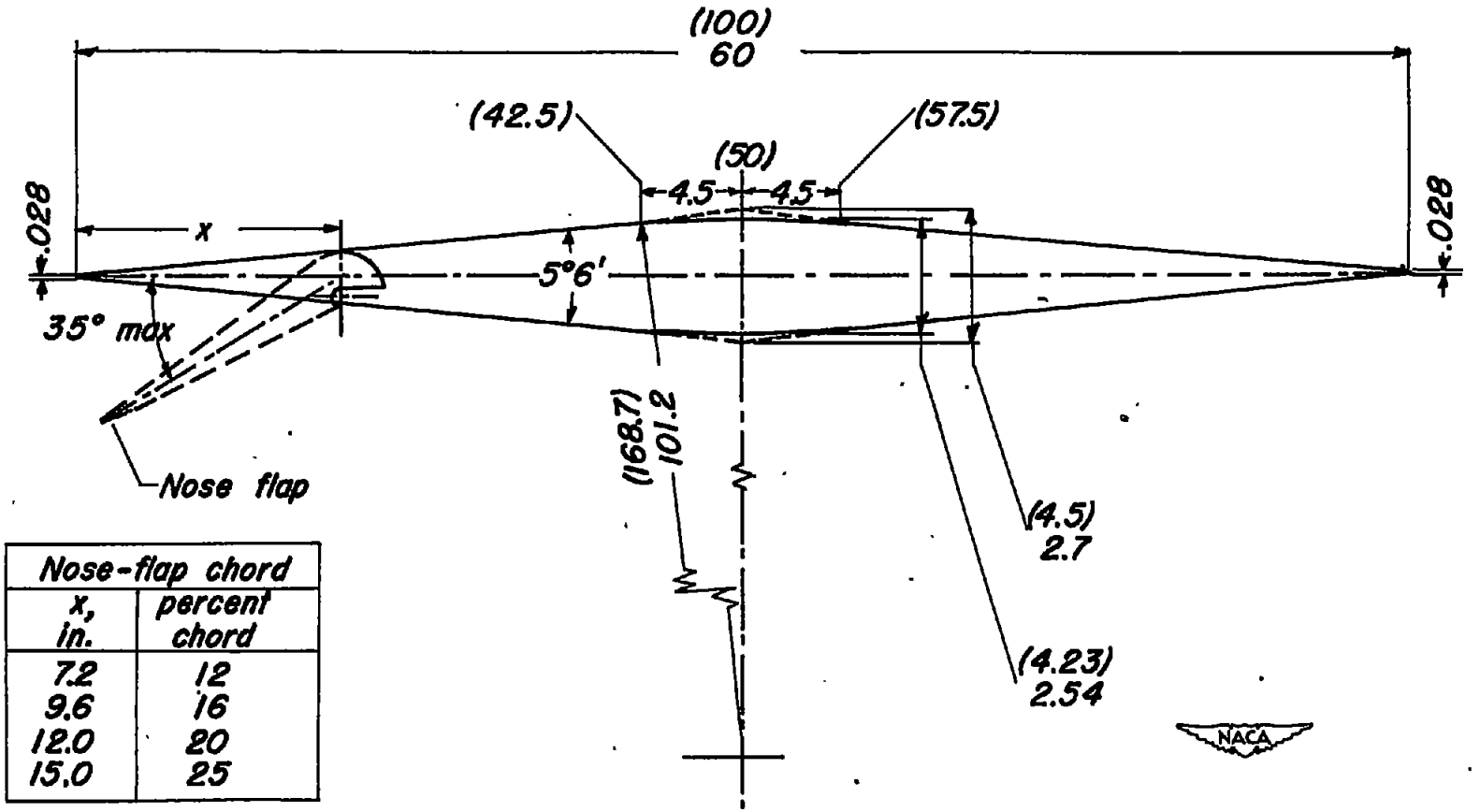

Nose-flap chord	
x, in.	percent chord
7.2	12
9.6	16
12.0	20
15.0	25

All dimensions in inches.
Numbers in parentheses denote percent chord.

Figure 1.—The faired, double-wedge airfoil with nose flap.

Figure 2.– The faired, double-wedge airfoil model installed in the wind tunnel showing the apparatus used to measure the velocity distribution above the upper surface.

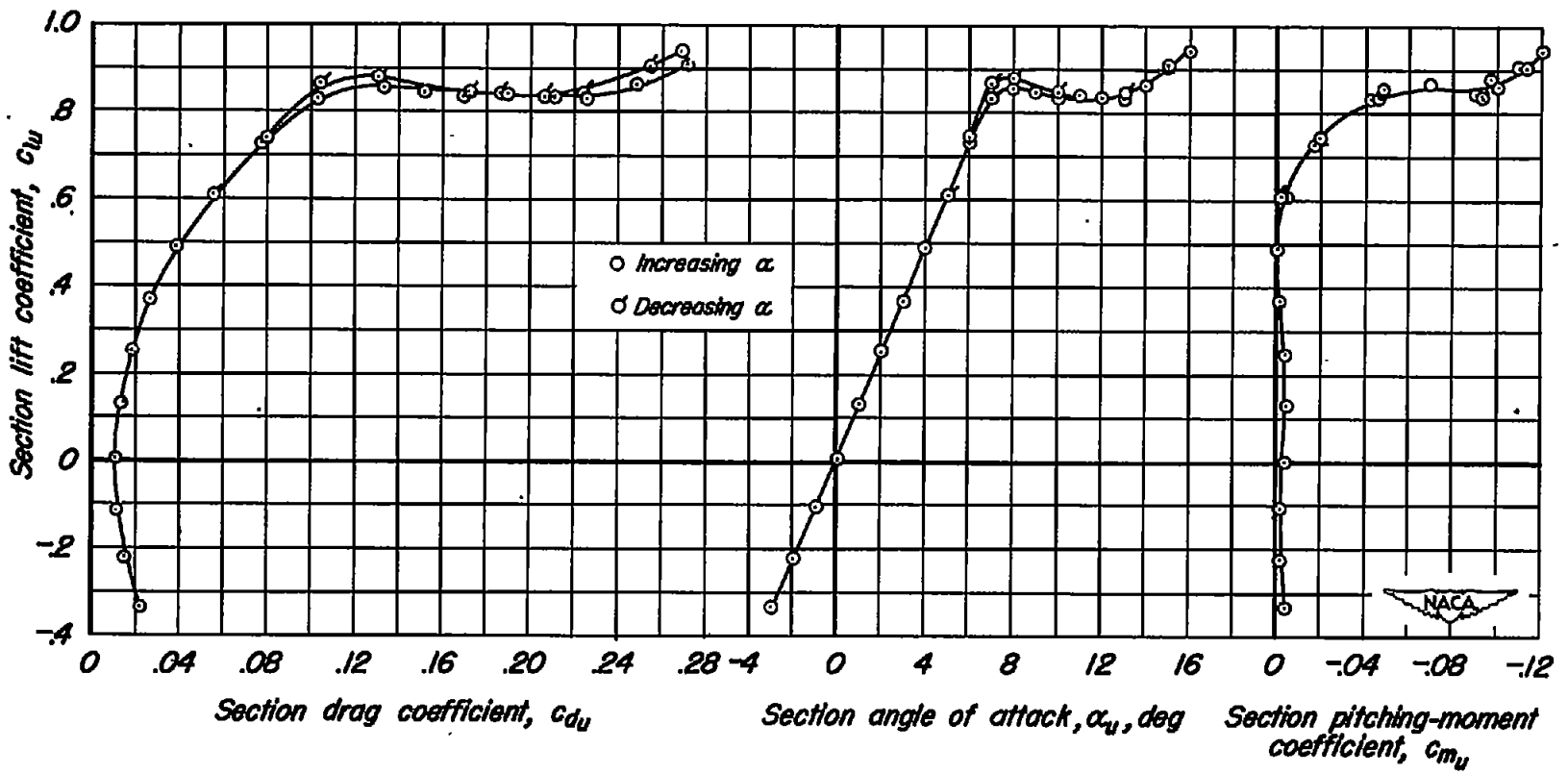

Figure 3.—Lift, drag, and pitching-moment characteristics for the basic airfoil.

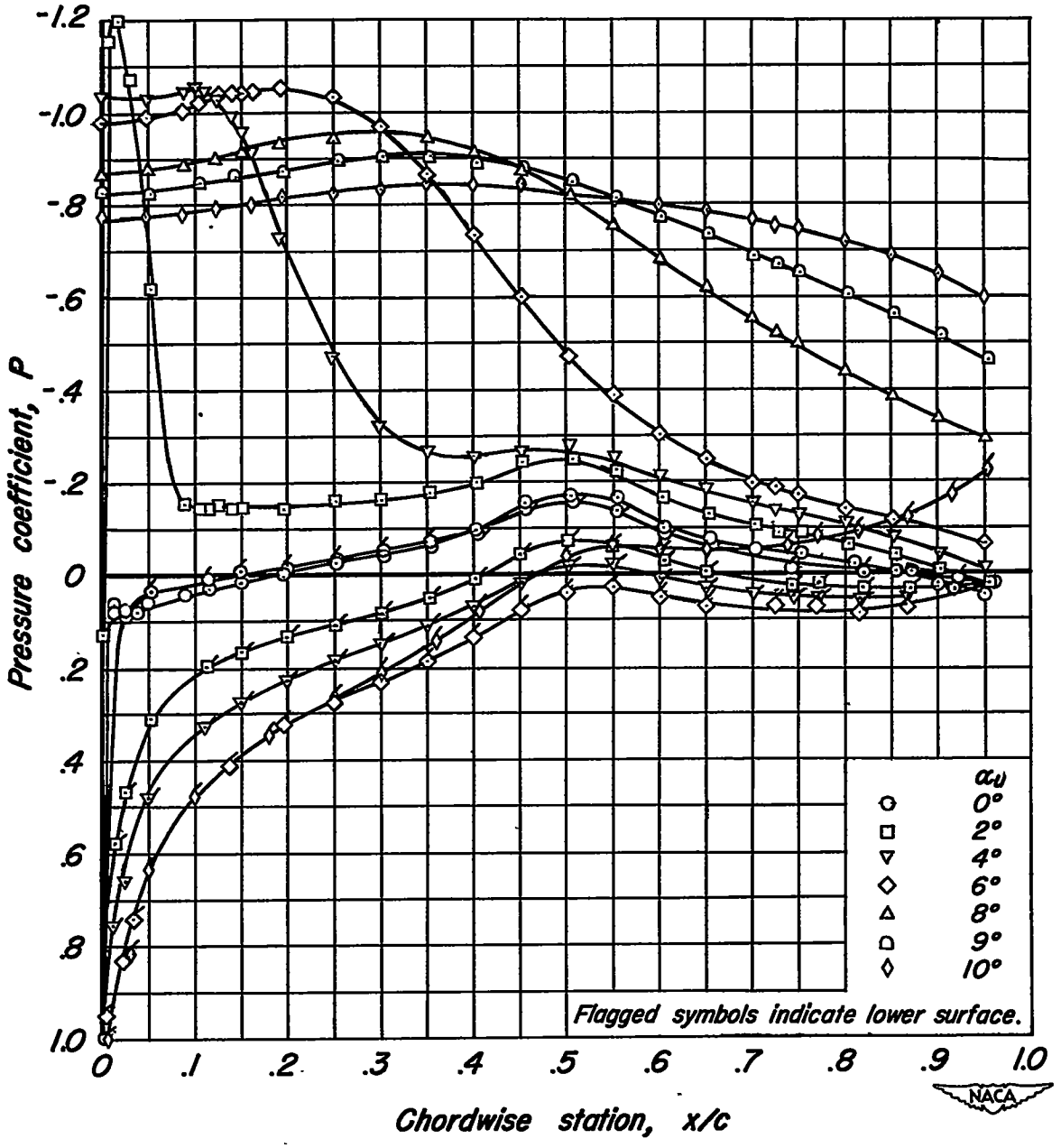

Figure 4.— Pressure distribution on the basic airfoil.

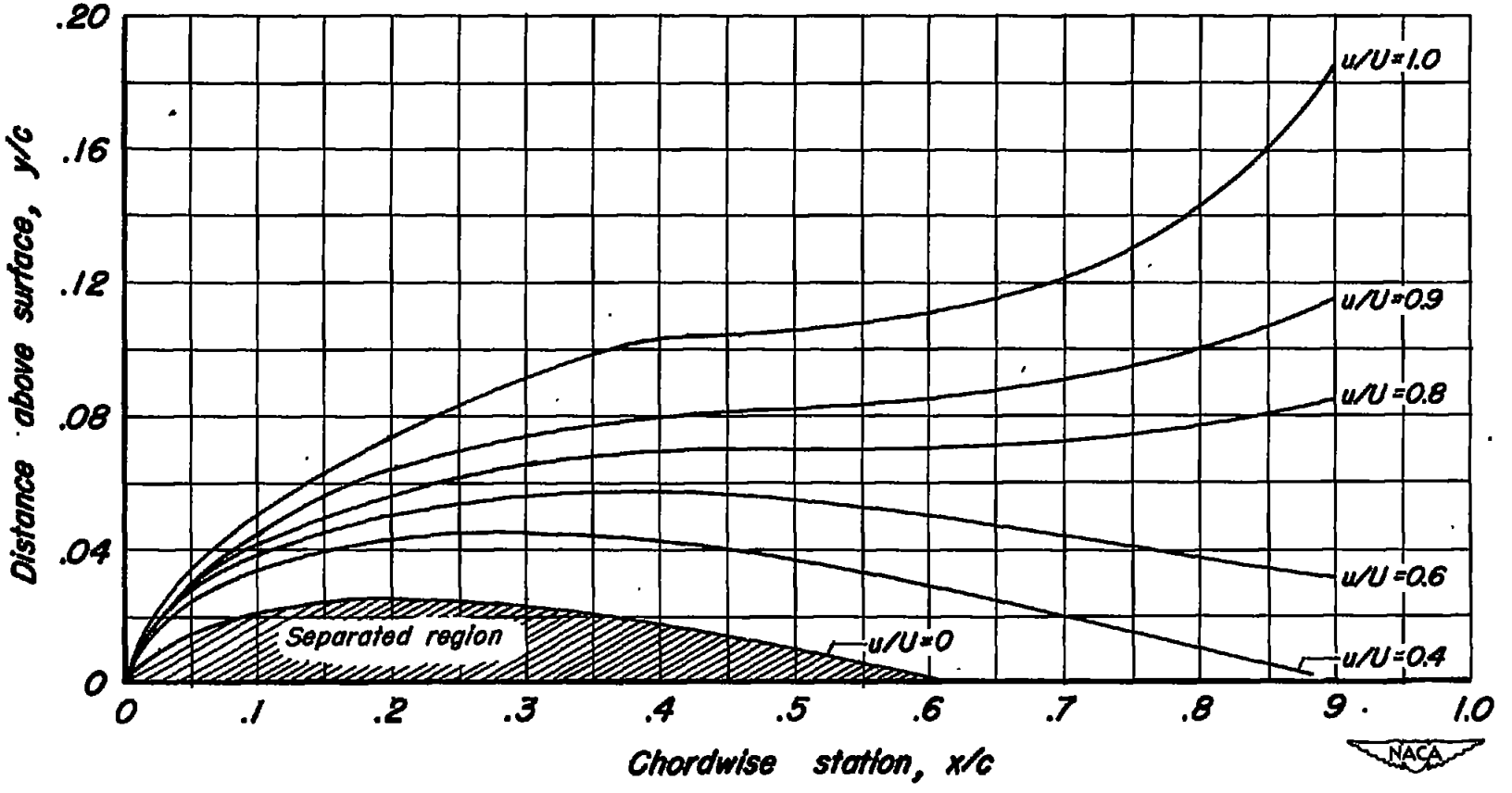

Figure 5.—Velocities above the basic airfoil at 6° angle of attack.

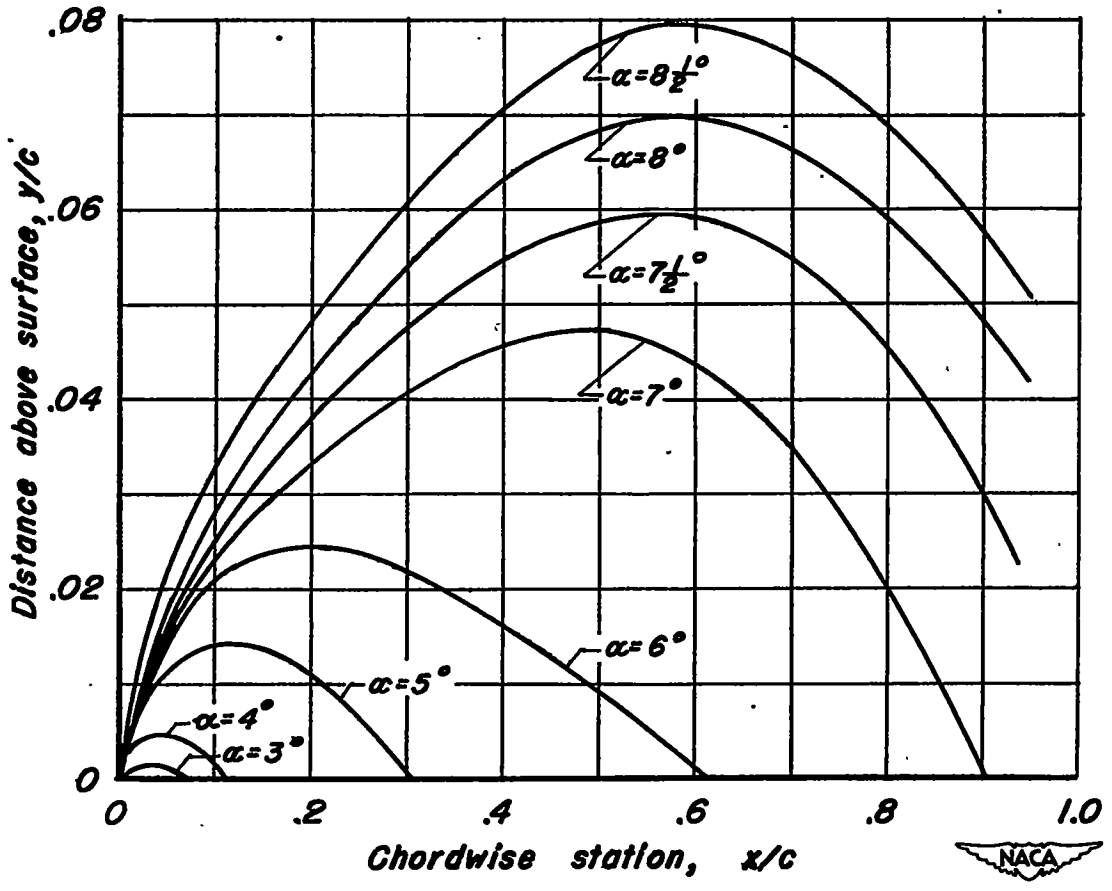

Figure 6.— The extent of the separated region for the basic airfoil.

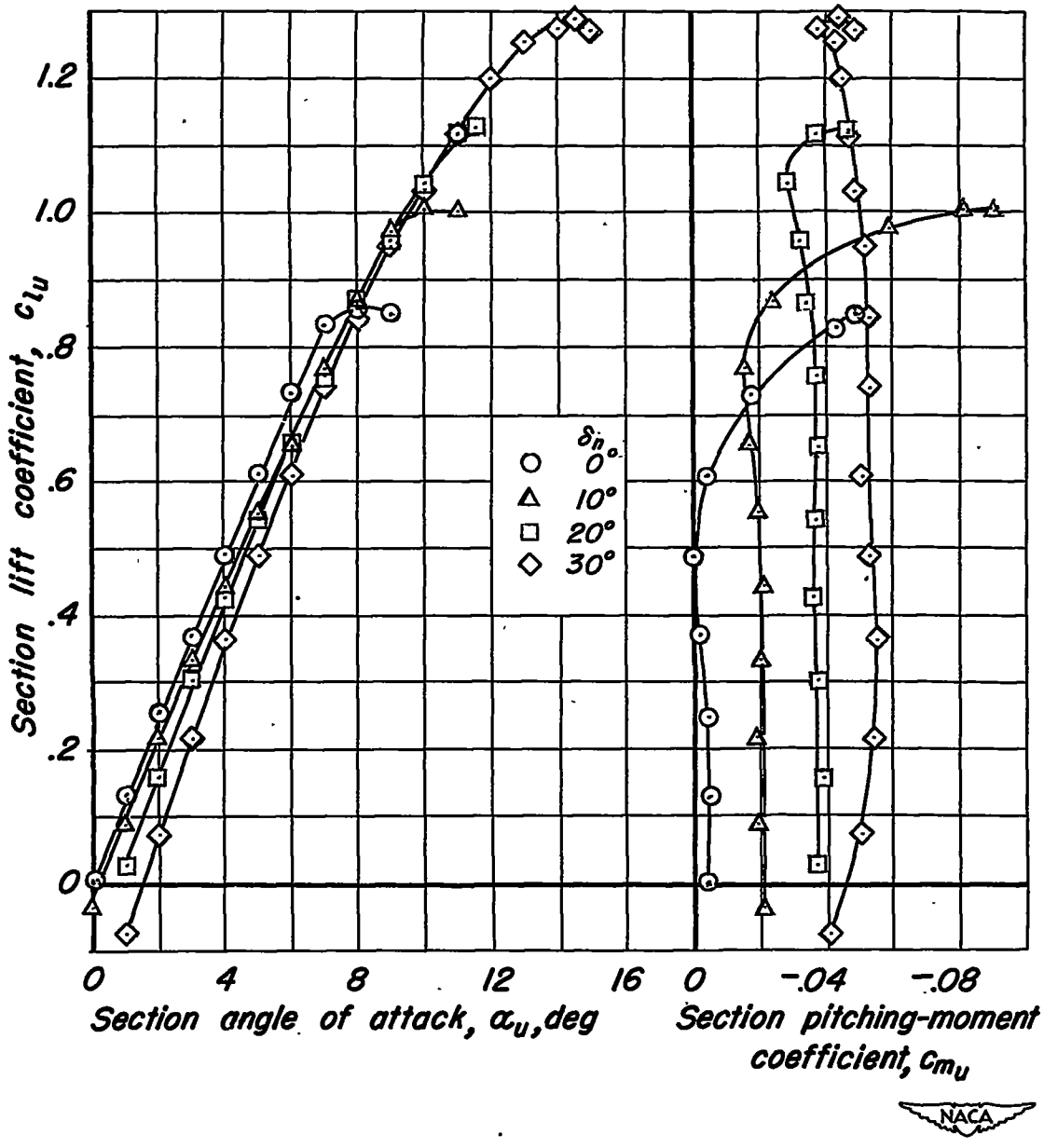

Figure 7.—Lift and pitching-moment characteristics of the airfoil with various flap deflections. 12-percent-chord nose flap.

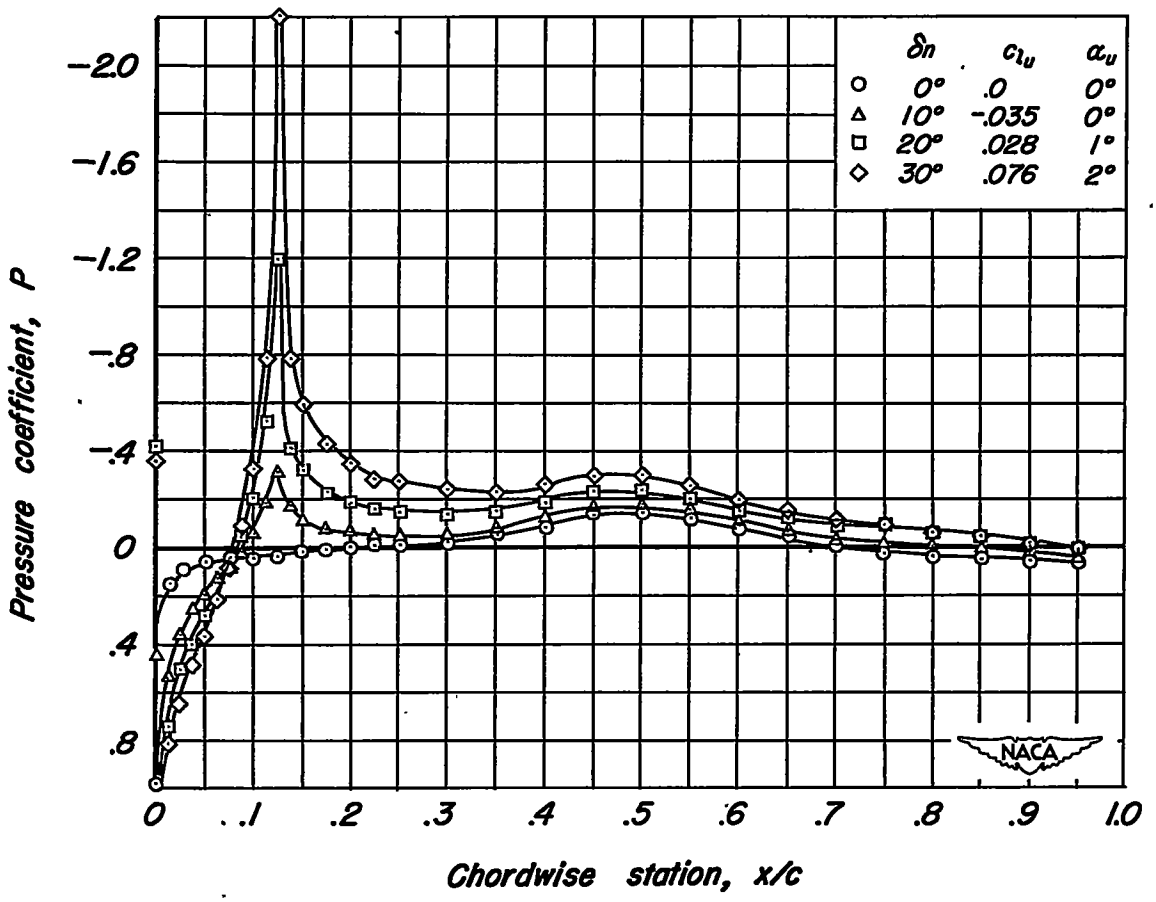

(a) $c_l = 0$ (approx.)

Figure 8.— Pressure distribution over the upper surface for various nose-flap deflections. 12-percent-chord nose flap.

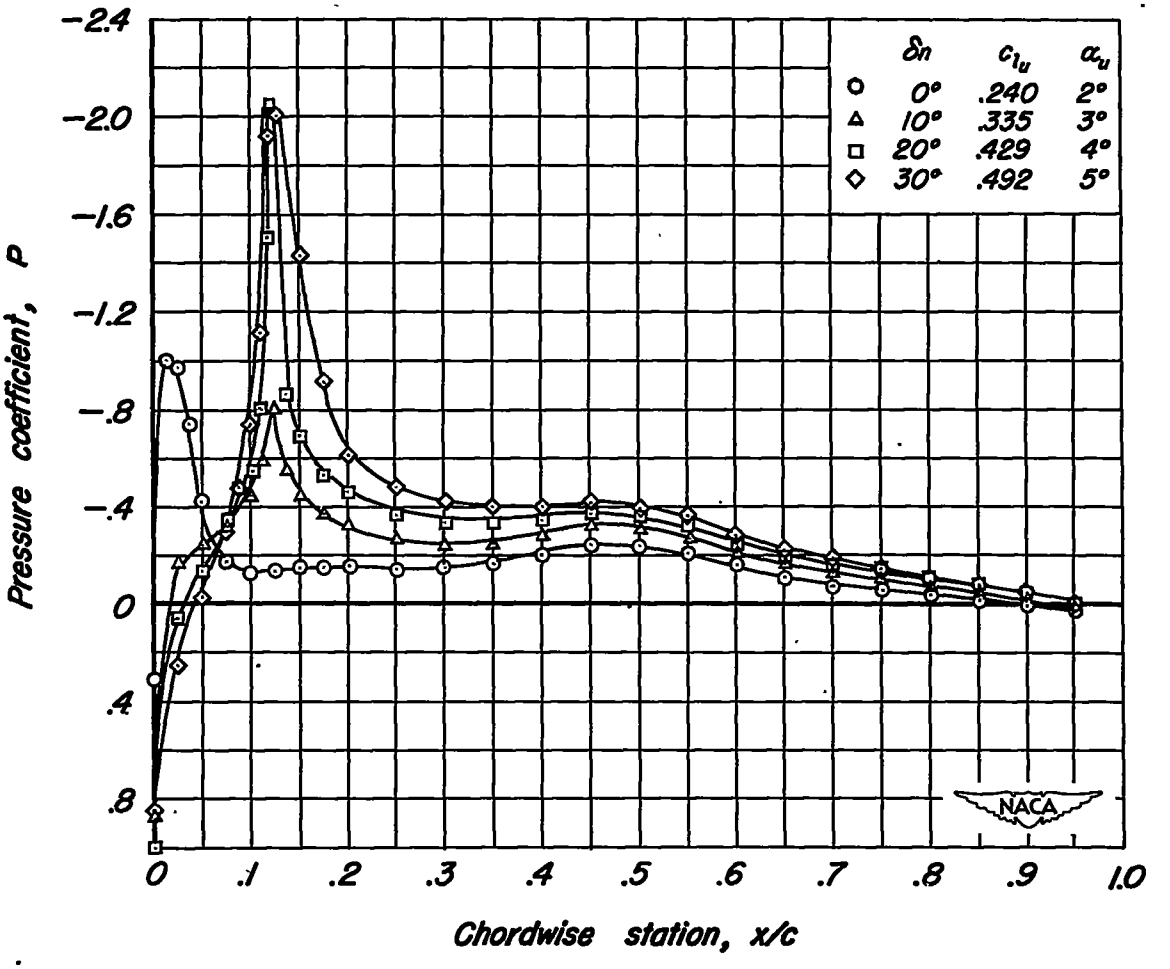

(b) $c_l = 1/3\, c_{l_{max}}$ (approx.)

Figure 8.—Continued.

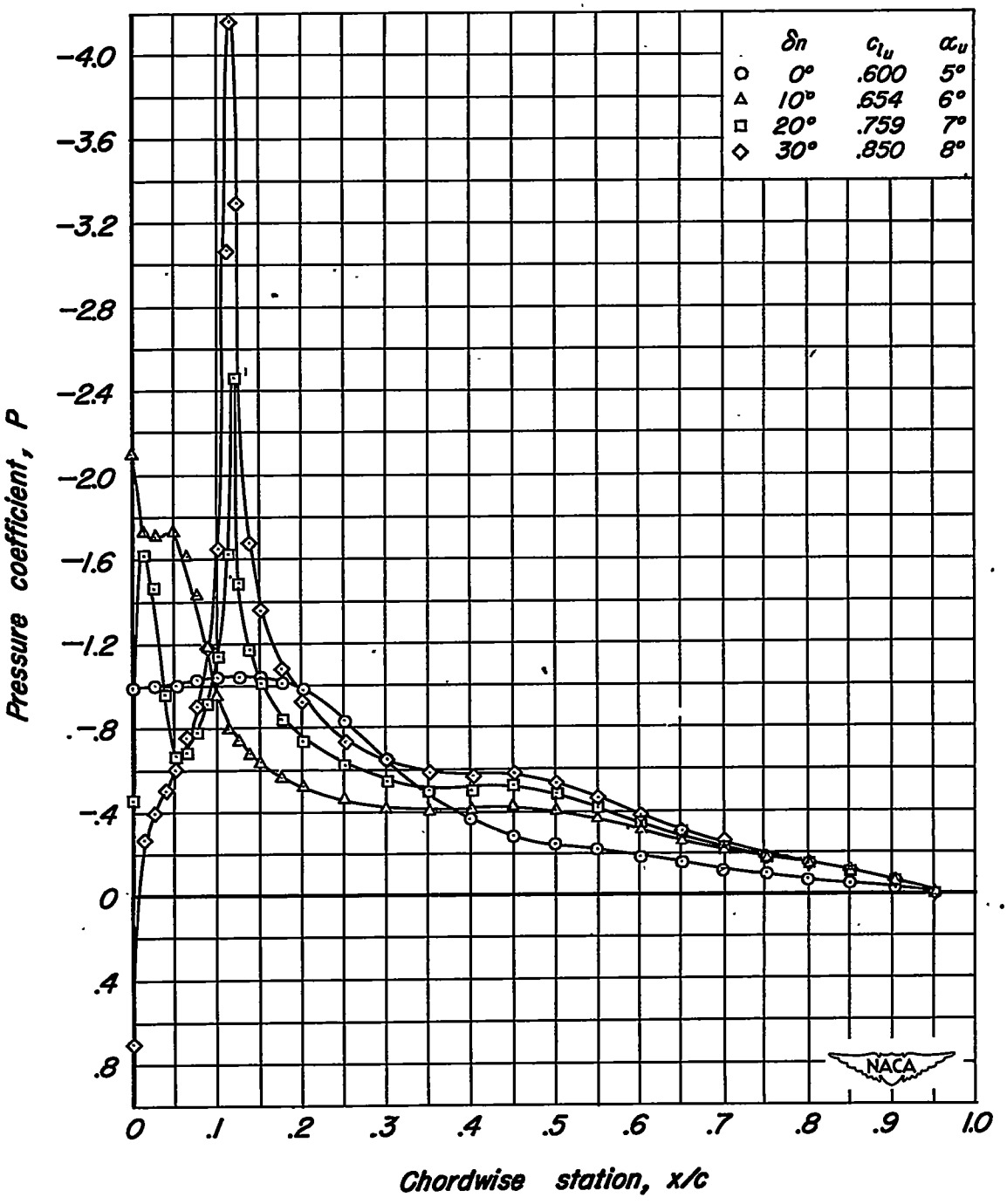

(c) $c_l = 2/3 c_{l_{max}}$ (approx.)

Figure 8.– Continued.

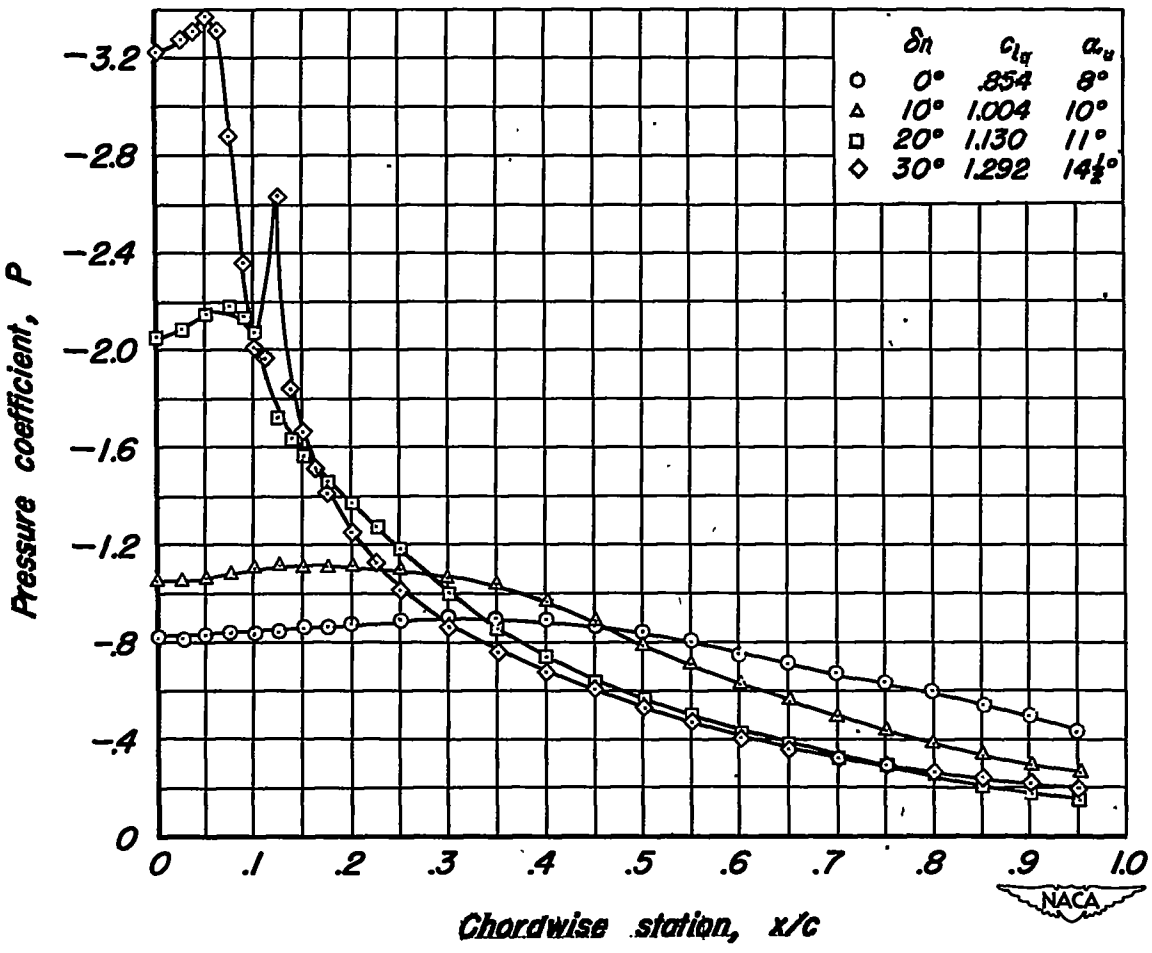

(d) $c_l = c_{l_{max}}$ (approx.)

Figure 8.—Concluded.

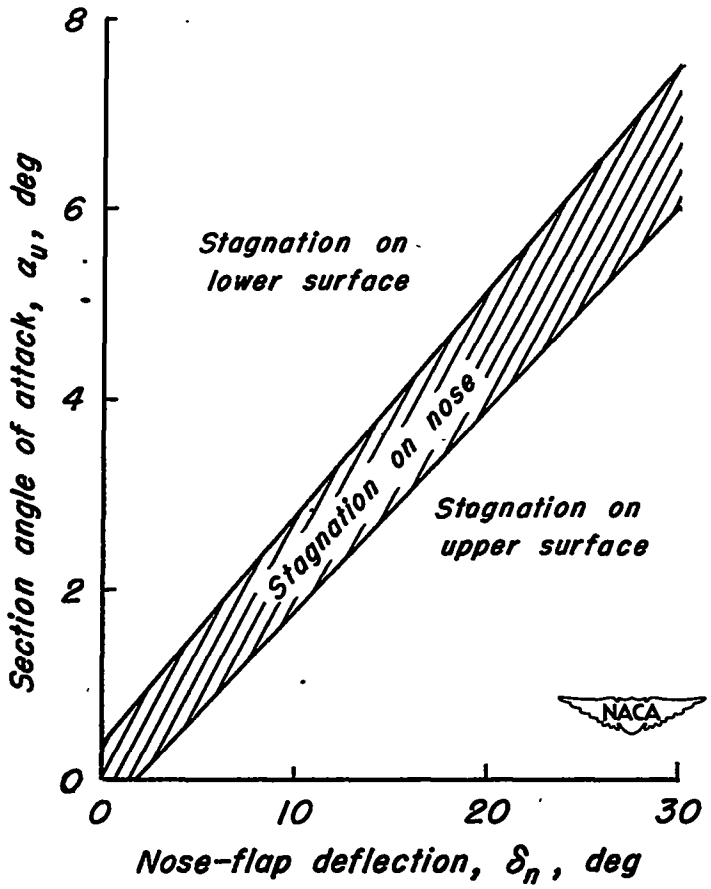

Figure 9.—The effect of nose-flap deflection on the location of the stagnation point. 12-percent-chord nose flap.

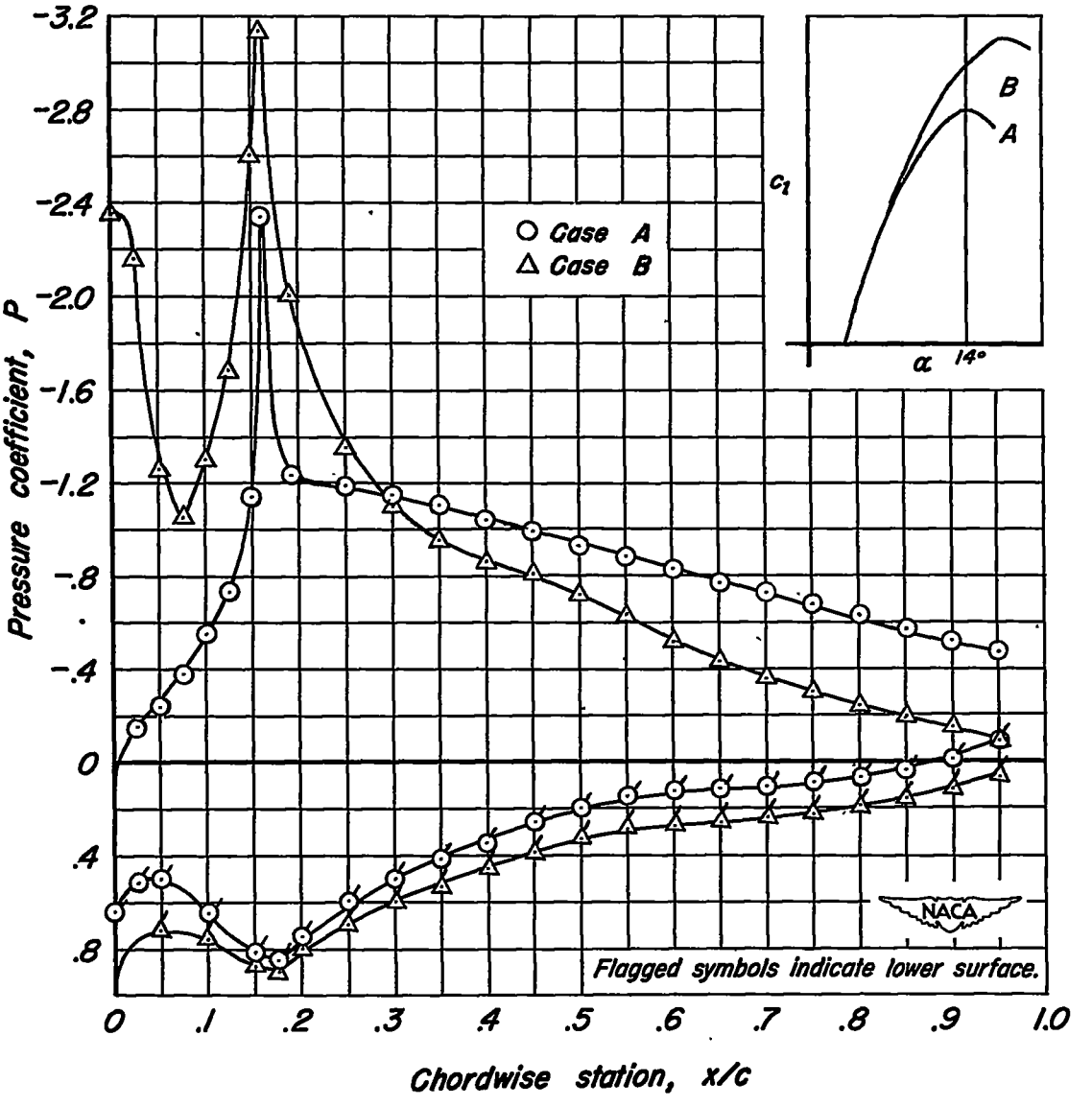

Figure 10.—Pressure distribution at 14° angle of attack with the nose flap deflected 35°. 16-percent-chord nose flap.

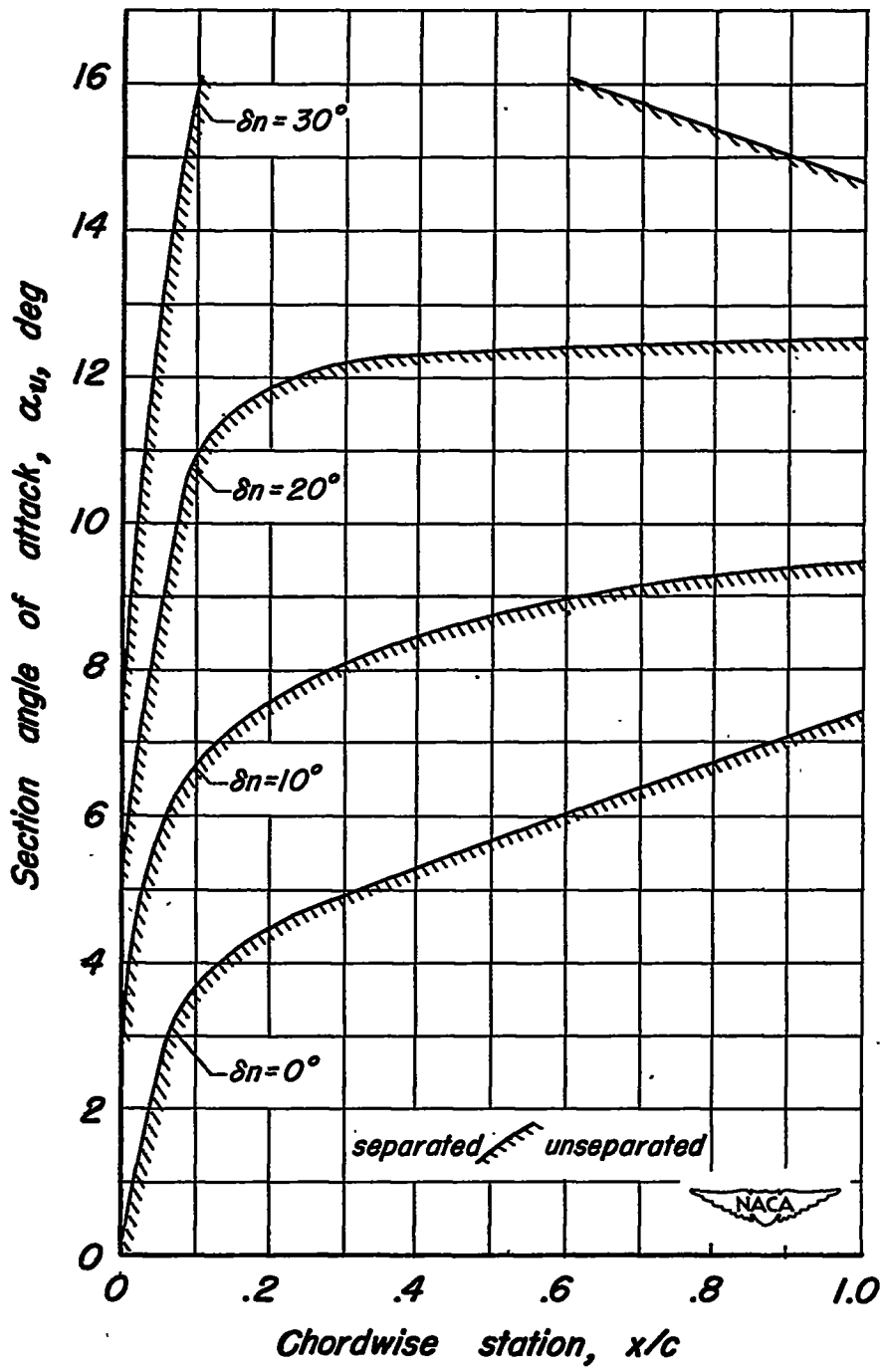

Figure 11.—The extent of the separated region for various nose-flap deflections. 12-percent-chord nose flap.

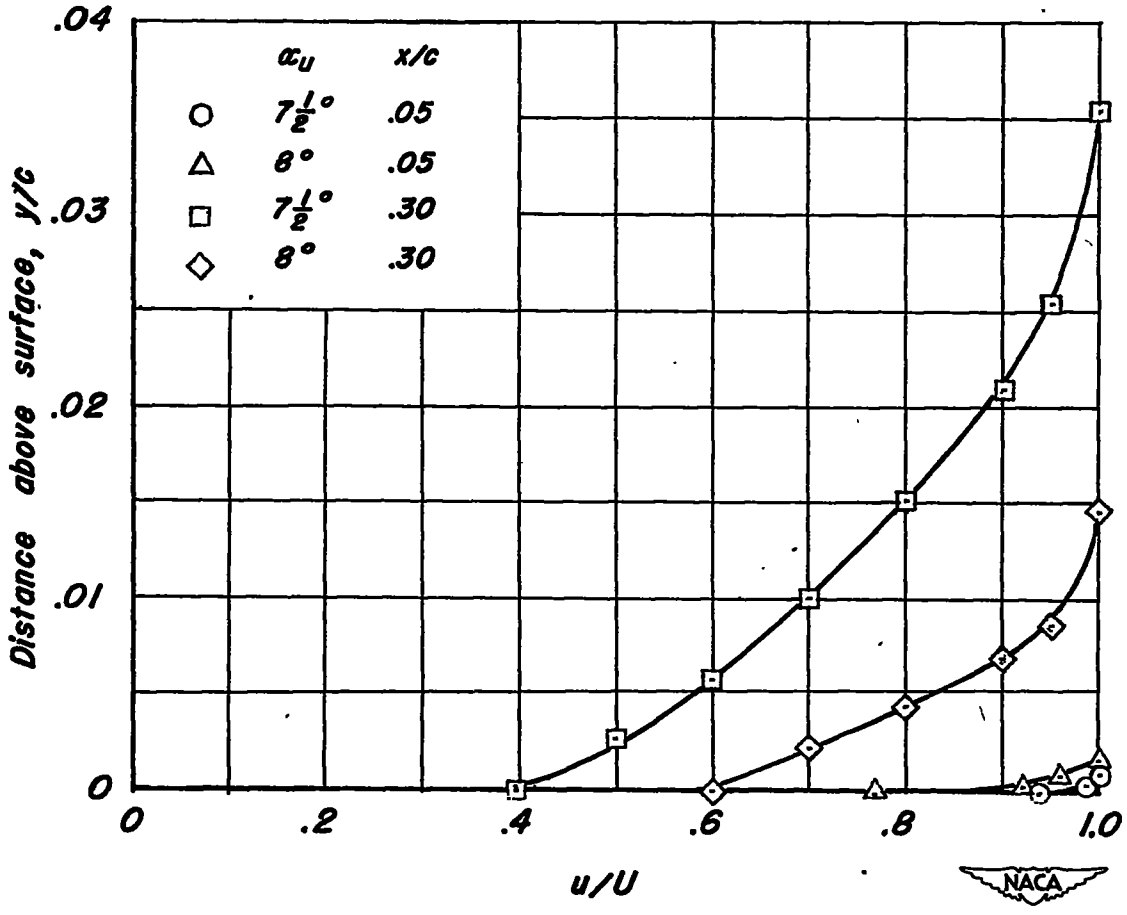

Figure 12.–Boundary-layer velocity profiles at two chordwise stations with the nose flap deflected 30°. 12-percent-chord nose flap.

NACA-Langley - 8-22-50 -925